

Energetics of the Phase Transition in Free-standing versus Supported Lipid Membranes

Agustin Mangiarotti, and Natalia Wilke

J. Phys. Chem. B, **Just Accepted Manuscript** • Publication Date (Web): 15 Jun 2015

Downloaded from <http://pubs.acs.org> on June 15, 2015

Just Accepted

“Just Accepted” manuscripts have been peer-reviewed and accepted for publication. They are posted online prior to technical editing, formatting for publication and author proofing. The American Chemical Society provides “Just Accepted” as a free service to the research community to expedite the dissemination of scientific material as soon as possible after acceptance. “Just Accepted” manuscripts appear in full in PDF format accompanied by an HTML abstract. “Just Accepted” manuscripts have been fully peer reviewed, but should not be considered the official version of record. They are accessible to all readers and citable by the Digital Object Identifier (DOI®). “Just Accepted” is an optional service offered to authors. Therefore, the “Just Accepted” Web site may not include all articles that will be published in the journal. After a manuscript is technically edited and formatted, it will be removed from the “Just Accepted” Web site and published as an ASAP article. Note that technical editing may introduce minor changes to the manuscript text and/or graphics which could affect content, and all legal disclaimers and ethical guidelines that apply to the journal pertain. ACS cannot be held responsible for errors or consequences arising from the use of information contained in these “Just Accepted” manuscripts.



1
2
3 **Energetics of the Phase Transition in Free-standing versus Supported Lipid**
4 **Membranes**
5
6

7 Agustín Mangiarotti and Natalia Wilke*

8
9
10 Centro de Investigaciones en Química Biológica de Córdoba (CIQUIBIC, UNC-
11 CONICET), Departamento de Química Biológica, Facultad de Ciencias Químicas,
12 Universidad Nacional de Córdoba, Argentina.
13

14
15 *Corresponding author at: Centro de Investigaciones en Química Biológica de
16 Córdoba (CIQUIBIC, UNC-CONICET), Departamento de Química Biológica,
17 Facultad de Ciencias Químicas, Universidad Nacional de Córdoba. Haya de la
18 Torre y Medina Allende, Ciudad Universitaria, X5000HUA, Córdoba, Argentina.
19 E-mail: wilke@mail.fcq.unc.edu.ar TE/FAX +54-351-5353855.
20
21
22
23
24
25
26
27
28
29
30
31
32
33
34
35
36
37
38
39
40
41
42
43
44
45
46
47
48
49
50
51
52
53
54
55
56
57
58
59
60

ABSTRACT

We compared the thermodynamic behavior of supported and free-standing films of phospholipids with different chain length and showed that the change in free energy for the phase transition to a denser state was greater in free-standing than in supported membranes, with the differences being independent of the chain length. The presence of the support promoted a decrease in the energy gap between the coexisting phases of 1.7 kJ mol^{-1} , and this was a long-range effect affecting both leaflets, probably related with the impediment of out-of-plane motion of the film by the solid surface.

1. INTRODUCTION

Model lipid membranes have been widely used in biophysical research to study processes that take place in the plasma membrane and inner cellular compartments. Langmuir monolayers, giant, large and small unilamellar along with multilamellar vesicles, solid supported monolayers and bilayers and free-standing planar bilayers has been used to study the texture and mechanical properties of membranes, membrane-protein interactions, drug penetration, along with other properties, with different kind of lipids. In the recent decades, with the development of biosensors and the advent of high-resolution techniques, supported lipid bilayers (SLBs) have gained increasing attention.^{1,2} SLBs also permit to reproduce biological membranes compositional asymmetry, and enable the inclusion of inorganic solids or polymeric materials.³⁻⁶ However, a full understanding of the influence of the preparation method and the nature of the solid substrate is still lacking. This knowledge is necessary for retrieving biologically relevant information and to fully exploit these model systems; with this understanding, it is possible to know in which manner the general trends observed in a given model can be extended to other models and to cellular membranes.

To this purpose, in a previous research we made a systematic comparison of the phase diagram for the DPPC/DLPC mixture in different model membrane systems and their thermodynamic properties were compared.⁷ The phase behavior in Langmuir monolayers, giant unilamellar vesicles, and supported monolayers and bilayers was quantified, and the results indicate that the properties of the expanded and the condensed phases become more similar when confining the lipidic system on glass supports, in agreement with results of other authors.⁸

To shed more light on this issue, we analyze here the energetics of the phase transition in free-standing (Langmuir monolayers) and supported membranes (bilayers on glass) for five phosphatidylcholines with different chain length with the aim of understanding the causes of the differences between the models studied before. The study was performed with binary mixtures of phospholipids with different hydrocarbon chain lengths that phase segregate in a wide compositional range. Here we show that knowing the phase diagrams of the mixtures, the change in chemical potential involved in the phase transition of pure lipids can be estimated and thereby, the properties of free-standing and supported films can be compared.

2. EXPERIMENTAL SECTION

2.1 Materials

The phospholipids 1,2-dilauroyl-sn-glycero-3-phosphocholine (DLPC), 1,2-dimirystoyl-sn-glycero-3-phosphocholine (DMPC), 1,2-dipalmitoyl-sn-glycero-3-phosphocholine (DPPC), 1,2-distearoyl-sn-glycero-3-phosphocholine (DSPC), 1,2-diarachidoyl-sn-glycero-3-phosphocholine (DAPC), and the lipophilic fluorescent probe L- α -Phosphatidylethanolamine-N-(lissamine rhodamine B sulfonyl) (Ammonium Salt) (Egg-Transphosphatidylated, Chicken) (PE-Rhoegg) were purchased from Avanti Polar Lipids (Alabaster, AL, USA).

Lipid mixtures were prepared in $\text{Cl}_3\text{CH}/\text{CH}_3\text{OH}$ 2:1 v/v to obtain a solution of 1nmol/ μL total concentration with all the solvents and chemicals used being of the highest commercial purity available. The subphase in all the experiments was deionized water with a resistivity of 18 M Ωcm , obtained from a Milli-Q Gradient System (Millipore, Bedford, MA).

The glass coverslips (12 mm diameter) used for the supported membranes were purchased from Marienfeld GmbH & Co. Kg (Germany).

2.2 Surface pressure-area measurements

Compression isotherms were taken on a commercial Langmuir balance (KSV minitrough, KSV Instruments, Ltd. Helsinki, Finland) measuring the surface pressure (π) by the Wilhelmy method with a platinum plate and recording the total film area while compressing at rates between 1 and 5 $\text{\AA}^2 \text{molecule}^{-1}\text{min}^{-1}$. Lipid mixtures of the desired composition were spread onto deionized water up to a mean molecular area higher than the lift-off area.

2.3 Preparation of supported membranes

Supported lipids bilayers were formed by transferring monolayers previously formed at the air-water interface onto hydrophilic cover-glasses using the Langmuir-Blodgett (LB) and Langmuir-Schaefer (LS) methods described in Mangiarotti et al. 2014.⁷ Briefly, the transfers were realized at a constant surface pressure of 30mN/m and a transfer rate of 5 mm/min, with the deposition of the first hemilayer by LB and the second one by LS transfer. The transfer ratio were always between 0.95 and 1.2, indicating that the monolayers were properly transferred to the glass substrate.⁹ The SLBs generated were asymmetric, since the first transferred film (the leaflet proximal to the glass surface) was made only of the component of the particular mixture with the longest hydrocarbon chain (DAPC, DSPC or DPPC) and in the absence of the fluorescent probe, while the second transferred film (the distal leaflet) contained the desired binary lipid mixture with 1 mol% of PE-Rhoegg (unless specified, see Table 1). Once the second monolayer was transferred, the covered glasses remained submerged in water during all the experiment. On the contrary, when only a monolayer was observed (see Table 1), the film remained in air.

2.4 Image acquisition and processing

Phase coexistence was visualized by Fluorescence Microscopy (FM). Images were acquired with an inverted fluorescence microscope Axiovert 200 (Carl Zeiss, Oberkochen, Germany) equipped with a CCD video camera iXON (Andor, Belfast, Northern Ireland) and 20x and 40x objectives. The fluorescent probe (PE-Rhoegg) was incorporated in the lipid solution before spreading (1 mole%).

In order to assess if the fluorescent probe had modified the phase behavior of the mixture, the results obtained with FM in monolayers at the air-water interface were compared with the images obtained with BAM, where no probe is required. For these experiments, the monolayers under compression were observed using an EP3 Imaging Ellipsometer (Accurion, Goettingen, Germany) with a 20x objective. The analysis and quantification of the images were carried out using Image J software as detailed in the supporting section of Caruso et al.¹⁰

3. RESULTS

3.1 Phase diagrams and composition of the coexisting phases.

All the lipid mixtures used in this work presented phase segregation in a wide range of compositions. In Langmuir monolayers (LMs), phase coexistence was followed using BAM and FM allowing the construction of a phase diagram for each lipid mixture, and thereby the determination of the phase boundaries (X^{LE} and X^{LC}) at all surface pressures.

As an example, Figure 1A shows the phase diagram for LMs composed of DSPC/DLPC. Micrographs obtained with FM ($X_{\text{DSPC}}=0.03$ and 0.20) and BAM ($X_{\text{DSPC}}=0.80$ and 0.97) at 30mNm^{-1} can be observed as insets. In BAM images the liquid-expanded (LE) phase corresponds to the darker areas and the liquid-condensed (LC) domains appear as lighter grey levels due to the higher refractive index and the larger thickness.¹¹ The opposite is observed in FM images, the lighter areas correspond to the LE phase since the probe is preferentially located there. The black circles in Figure 1 A indicate the surface pressure for the boundaries between regions with LE/LC phase coexistence and a homogeneous LE film, the diamond shape indicates the border between LC/LE phase coexistence and a homogeneous LC film, and the white circles correspond to the collapse pressure of the film. The dotted line indicates the surface pressure at which the monolayers and the supported bilayers have been compared (i.e. the film transference onto the solid was made at 30mNm^{-1}). The values of X^{LE} and X^{LC} (compositions of the LE and the LC phases, i.e. compositions of the border of the regions with phase coexistence) at 30mNm^{-1} were 0.03 and 0.97 respectively for monolayers composed of DSPC/DLPC. These phase boundaries were shifted in SLBs as shown in Figure 1B, being $X^{\text{LE}}=0.04$ and $X^{\text{LC}}=0.75$. Note that to determine the composition at which the film was in a LC state in Langmuir monolayers BAM was used, allowing a clear detection of the coalescence of the phases, while for SLBs, only FM can be used. The incorporation of a fluorescent probe hindered the visualization of the composition at which the transferred film was completely in a LC state since the probe preferentially located in the LE phase, but when an homogeneous condensed state was reached, the resulting FM images were not homogeneous and regions where the probe remained appeared lighter resulting in an inhomogeneous texture (see micrographs for $X_{\text{DSPC}}=0.75$ and 0.90). Therefore, this boundary was determined in supported films as the lipid proportion at which the appearance of the image and the area occupied by the fluorescent regions showed no further changes as the lipid proportion changed.

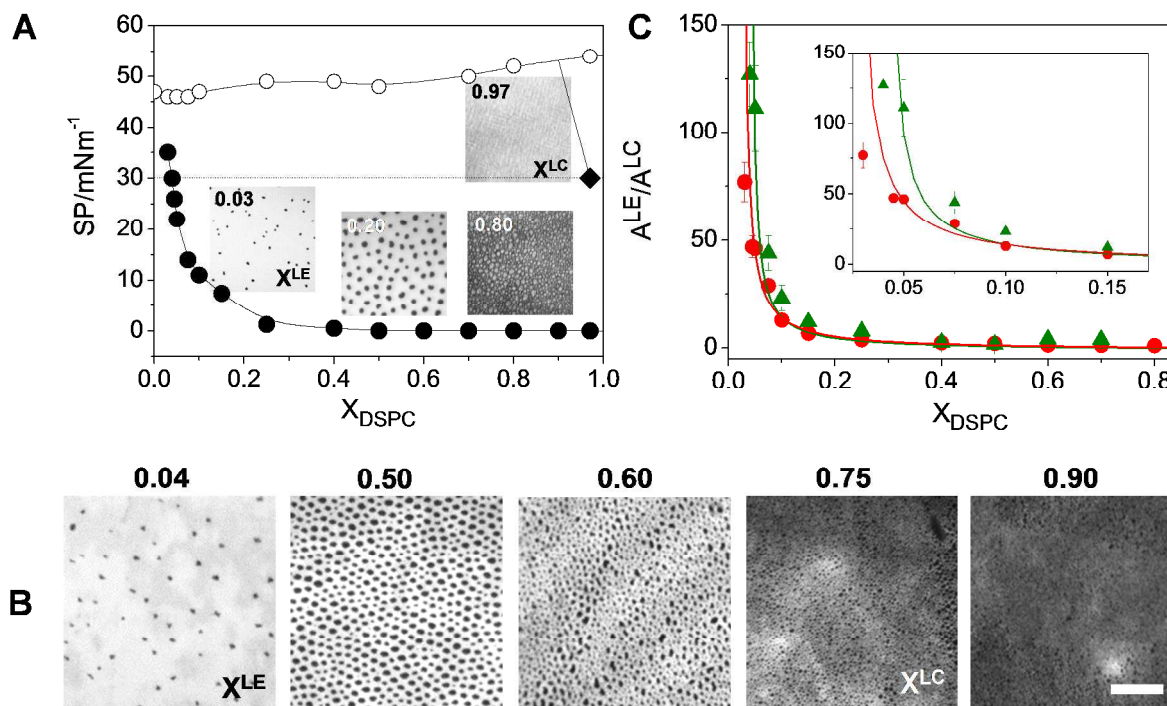


Figure 1. (A) Phase diagram (Surface Pressure vs. X_{DSPC}) for Langmuir Monolayers composed of DSPC/DLPC at $(22 \pm 1)^\circ\text{C}$. Borders of the two phase regions determined with BAM or FM: boundary between LC/LE and LE (●); boundary between LC/LE and LC (◆); and collapse pressure of the film (○). The dotted line indicates the surface pressure of transference, at which the free-standing and supported films were compared ($\text{SP} = 30 \text{ mN/m}$). Insets: representative micrographs taken with FM ($X_{\text{DSPC}} = 0.03$ and 0.20 , $400 \times 400 \mu\text{m}^2$) and BAM ($X_{\text{DSPC}} = 0.80$ and 0.97 , $150 \times 150 \mu\text{m}^2$). (B) Images of DSPC/DLPC supported bilayers transferred by the LB-LS method taken with FM under water (Images size: $400 \times 400 \mu\text{m}^2$, the scale bar is $100 \mu\text{m}$). For both systems X_{DSPC} and the values of X^{LE} and X^{LC} are indicated. (C) Area ratio ($A^{\text{LE}}/A^{\text{LC}}$) vs X_{DSPC} for LMs (●) and SLBs (▲) together with the calculated curves for the lever rule: $A^{\text{LE}}/A^{\text{LC}} = (a^{\text{LE}}/a^{\text{LC}}) \times (x^{\text{LC}} - x)/(x - x^{\text{LE}})$, where a^{LE} and a^{LC} are the mean molecular areas of the LE and LC phases, obtained from the compression isotherms at the compositions of the corresponding boundaries. Inset: scale magnification showing the differences between the systems.

The ratio between the area percentages of LE phase to LC phase for a particular lipid composition in a phase segregated system relates with the phase diagram of the mixture through the lever rule; the composition and general properties of the phases in coexistence do not change over the whole range of phase segregation at constant temperature and surface pressure. All the mixtures used in this research followed the lever rule, as exemplified in Figure 1C for the DSPC/DLPC mixture in free-standing and supported systems.

In a previous work, we showed that the composition of the phases in supported bilayers composed of DPPC and DLPC is the same for the leaflet distal and for that proximal to the support, indicating that there is no influence of the possible short-distance interactions between the glass and the lipids on the phase segregation of this lipid mixture.⁷ In addition, the phase boundaries of monolayers compared to bilayers both in free-standing and supported models (Langmuir monolayers vs. giant unilamellar vesicles and supported monolayers vs. supported bilayers) are similar; indicating that inter-leaflet interactions do not markedly affect the phase diagram of this lipid mixture.⁷

In order to check whether this is a general observation in phospholipid films absorbed on glass, we analyzed here the areas occupied by the expanded and the condensed phases for other two mixtures. Table 1 summarizes the results obtained for DAPC/DMPC (a chain difference of 4 carbons) and DSPC/DLPC (6 carbons of difference). The area ratios remained the same for supported bilayers when the hemilayer containing the lipid mixture was transferred first (proximal to the support) or when it was the distal one, meaning that the observed compositions were not affected by flip-flop and that the results shown here can be considered valid for both leaflet. Even in the absence of the second hemilayer (i.e. supported monolayers) the area ratios remained the same, indicating that inter-leaflet interactions were not modifying the phase diagram of the lipid mixtures used in this work.

Table 1. Area fractions for different mixtures in the distal (dSLBs) and the proximal (pSLBs) leaflets of supported bilayers and for supported monolayers (SLM). In dSLB, the proximal hemilayer is composed of pure DAPC or DSPC while in pSLB, the distal hemilayer is composed of pure DAPC or DSPC. SLM were observed in air and the bilayers under water.

A^e/A^c	DAPC/DMPC	DSPC/DLPC
	$X_{\text{DAPC}}=0.07$	$X_{\text{DSPC}}=0.25$
dSLBs	38±7	7±1
pSLBs	35±5	5±2
SLM	33±5	6±1

The compositions of the phases in coexistence were determined for five binary lipid mixtures as explained above. The obtained values are given in Table 2 where it can be observed that the range of phase coexistence was always smaller when the system was confined, i.e. the lipids were more miscible in the presence of the support. However, a clear tendency cannot be described, since the boundaries were shifted in different proportions for each mixture and therefore, other parameter has to be analyzed for a more quantitative comparison; this is performed in the next section.

Table 2. Composition of the phases in coexistence in binary phospholipid mixtures for free-standing and supported membrane systems.

Lipid mixture	LMs		SLBs	
	X^{LE}	X^{LC}	X^{LE}	X^{LC}
DPPC/DLPC	0.170 ± 0.007	0.95 ± 0.04	0.35 ± 0.01	0.90 ± 0.04
DSPC/DMPC	0.080 ± 0.003	0.92 ± 0.04	0.120 ± 0.005	0.80 ± 0.03
DSPC/DLPC	0.030 ± 0.001	0.90 ± 0.04	0.040 ± 0.002	0.75 ± 0.03
DPPC/DMPC	0.40 ± 0.02	0.85 ± 0.03	0.45 ± 0.02	0.80 ± 0.03
DAPC/DMPC	(50±2)10 ⁻⁴	0.96 ± 0.04	(100±4)10 ⁻⁴	0.87 ± 0.03

The indicated X^{LE} and X^{LC} values correspond to the longest lipid of each mixture.

3.2 Calculation of the free energy of the phase transition.

In the regions where the LE and the LC phases coexist in equilibrium, the chemical potential of each lipid i in each phase is the same, i.e.:

$$\mu_i(LC) = \mu_i(LE) \quad (1)$$

All the selected lipid mixtures showed low miscibility (as shown in Fig. 1 for DSPC/DLPC), and therefore, each phase in coexistence was a mixture in which one of the components was in a very small proportion. Thus, the chemical potential of each lipid in each phase can be considered as that for ideal mixtures:

$$\mu_i(LC) = \mu_i^\phi(LC) + RT \ln(x_i^{LC}) \quad (2)$$

$$\mu_i(LE) = \mu_i^\phi(LE) + RT \ln(x_i^{LE}) \quad (3)$$

Then, using eq. 1 to 3:

$$\mu_i^\phi(LC) + RT \ln(x_i^{LC}) = \mu_i^\phi(LE) + RT \ln(x_i^{LE})$$

$$\Delta\mu_i^{\phi, LC-LE} = RT \ln\left(\frac{x_i^{LE}}{x_i^{LC}}\right) \quad (4)$$

Equation 4 indicates that the chemical potential difference for the phase transition LE→LC of a pure lipid ($\Delta\mu$ from now on, for simplicity) can be estimated from the compositions of the phases in coexistence in a given binary mixture provided they can be considered as ideal mixtures, which is a good approximation when the components exhibit a low solubility since in that case, both phases correspond to dilute solutions. Furthermore, the compositions of the coexisting

phases in membranes are easily obtained by observing the presence or absence of micro-domains, as explained in the previous section.

Using eq. 4 and the compositions shown in Table 2, the chemical potential difference involved in the phase transition from liquid expanded to liquid condensed phase was calculated for the phosphatidylcholines with different chain length (from 12 to 20 carbons) in free-standing (LMs) and supported films (SLBs) at $(22\pm 1)^\circ\text{C}$ and at a surface pressure of 30mNm^{-1} . Two $\Delta\mu$ values were obtained from each mixture, corresponding to the phase transition of the pure lipids that composed it. For some lipids we obtained more than one value of $\Delta\mu$ (both free-standing and supported), since more than one mixture was analyzed for those lipids, as indicated in Table 3. It is important to remark that for those lipids, the different values of $\Delta\mu$ were similar, regardless of the mixture used for the determination, which indicates that considering ideal mixtures was a valid approximation. As expected, for a lipid with less than 16 carbons in their hydrocarbon chains the change of energy was positive for the phase transition, i.e. these lipids were stable in a LE phase at 22°C and 30mN/m . The opposite behavior was observed for lipids with longer chains. For DPPC, the values were in agreement with the reported Gibbs free energy calculated in monolayers using a different approach.¹²

Table 3. Chemical potential difference for the LE to LC transition in free-standing and supported systems.

Lipid	Mixed with	LMs $\Delta\mu$ (kJmol ⁻¹)	SLBs $\Delta\mu$ (kJmol ⁻¹)
DLPC	DPPC	6.9±0.5	4.6±0.5
	DSPC	5.6±0.5	3.3±0.5
DMPC	DPPC	3.4±0.5	2.5±0.5
	DSPC	6.0±0.5	3.6±0.5
	DAPC	7.9±0.5	5.0±0.5
DPPC	DLPC	-4.2±0.5	-2.3±0.5
	DMPC	-1.8±0.5	-1.4±0.5
DSPC	DLPC	-8.3±0.5	-7.2±0.5
	DMPC	-6.0±0.5	-4.7±0.5
DAPC	DMPC	-12.9±0.5	-11.0±0.5

A maximum error of 0.5 was assigned to $\Delta\mu$ values derived from the error in the concentration of the solutions containing the lipid mixtures and from independent experiments in the determination of X^{LE} and X^{LC} values.

In Figure 2A the data shown in Table 3 are plotted versus the lipid chain length for the different phosphatidylcholines used. Two major conclusions can be obtained from this graphic: firstly, there was a correlation between the chain length and the $\Delta\mu$ values for lipids with more than 16 carbons, becoming more negative as the chain length increased. On the contrary, for shorter lipids the contribution of the chain to the energetics of the phase transition was negligible, suggesting that for these lipids other factors different to the melting of the hydrocarbon chains (such as the polar head group and/or the hydration water), were dominating the process.

Secondly, in all cases the $\Delta\mu$ for the transition in supported systems was lower than that corresponding to free-standing systems; note that the black columns are closer to zero than the grey ones for each lipid. In other words, the phases became energetically more similar when the film was supported in all the analyzed lipids.

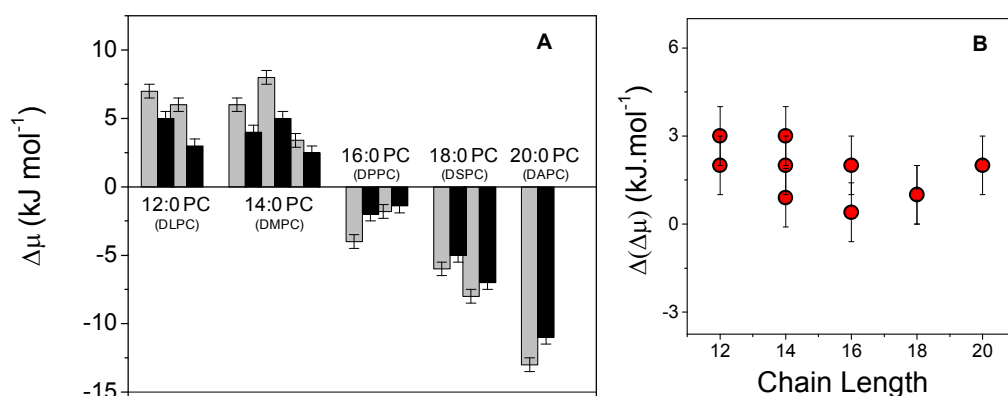


Figure 2. A. Chemical potential difference for the phase transition from the liquid expanded state to the liquid condensed state in Langmuir monolayers (grey bars) and supported lipid bilayers (black bars) for phosphatidylcholines with increasing chain length at $(22\pm 1)^\circ\text{C}$ and 30mNm^{-1} . **B.** Absolute value of the difference between the $\Delta\mu$ values for films in LMs and SLBs as function of the chain length.

Interestingly, the difference in the energetic cost for the phase transition in SLBs and LMs was independent of the particular lipid. In Figure 2B, the absolute value of the difference in the $\Delta\mu$ values of LMs and SLBs is plotted. On average, the phase transition in supported systems cost $(1.7\pm 0.8) \text{kJ mol}^{-1}$ less than for free-standing systems.

4. DISCUSSION

In all the analyzed mixtures, the region of phase coexistence decreased in the presence of the solid support. From the composition of the coexisting phases we were able to estimate the energetic cost for the phase transition for the pure lipids. Our main result show that in supported bilayers the energy required to change the phase state in membranes composed of different phospholipids was lower than for free-standing systems, and thus, in SLBs the phases were more similar than in LMs, explaining the increased miscibility of rigid lipids with less packed lipids when a mixture was analyzed. Interestingly, this reduction in energy was independent of the chain length, thus indicating that it was not related with a loss in the degrees of freedom of the hydrocarbon chain. The decrease in the free energy change supports previous findings regarding the phase behavior of DPPC/DLPC mixtures in free-standing (monolayers and giant unilamellar vesicles) and supported films (monolayers and bilayers on glass) in which the phase diagram of all supported membranes is shifted with respect to all free-standing systems, with an expanded phase richer in DPPC when the membrane is supported.^{7,8}

Similar values for the ratio of the areas of the coexisting phases were found when the distal hemilayer was observed, which according to the lever rule implies a similar composition of the coexisting phases and thus, similar energy change for the phase transition of the pure lipids (see Table 1 for DAPC, DMPC, DSPC and DLPC and ref. 7 for DPPC). Therefore, the glass surface did not promote further effects related with short-distance specific interactions and our observations appear to be a consequence of long-range effects observed in both leaflets. Furthermore, when a single monolayer was transferred, similar results than for supported bilayers were found, thus discarding the influence of inter-layer interactions on the phase diagram.

In free-standing membranes, out-of-plane fluctuations are possible, with amplitudes depending on the membrane bending modulus.¹³ In the case of lipid monolayers at the oil-water interface, it has been shown that the value of the mean bending modulus is similar to that on bilayers¹⁴ In Langmuir monolayers, while a flat geometry at the interface is observed in the micrometer scale, thermal undulations at the nanometer scale occurs, with growing amplitude upon reduction of the surface tension.¹⁵ These undulations lead to a smearing in the density profiles obtained with x-ray structures of about 0.4 nm¹⁶, higher than the clean air-water interface roughness (0.32 nm¹⁷) and comparable to those found in lipid bilayers.¹⁸

In supported lipid films, a 0.5-2 nm thick water layer has been determined between the polar-headgroup and the solid surface.¹⁹⁻²¹ This confined water is more structured than bulk water, showing ice-like peaks in the infrared spectra.²¹ Furthermore, it has been shown that due to the confining wall there is an increase in the effective viscosity of the fluid in this layer.²²

1
2
3 Therefore, the film undulations are expected to be markedly reduced when
4 confining the membrane to a solid support, as predicted by computational
5 simulations of SLBs that show compressibility changes with respect to free-
6 standing systems along with localization of the lipid molecules.²³
7

8 All this suggests that the confinement imposed by the solid surface leads to
9 the localization of the membrane and to restrictions in out-of-plane undulations.
10 The consequences of the restricted motion on the membrane are expected to be
11 higher in the expanded phase than in the condensed phase, thereby decreasing
12 the energy gap between the phases.
13

14 It has been proposed that the loss of entropy due to limited movement of
15 lipid molecules out of the plane of the membrane in SLBs play a main role in the
16 energy differences between free-standing and supported films.^{8,24–27} However, the
17 reduction in free energy described here maybe related not only with a loss of
18 entropy, but also with a decrease in enthalpy due to different intermolecular
19 interactions in the free standing compared to the supported film.
20

21 The value of the melting temperature ($T_m = \Delta H/\Delta S$ at the melting point) is
22 expected to increase if the entropy diminishes provided that the enthalpy of the
23 phase transition remains constant. Since the first explorations of SLBs, the value of
24 T_m for supported DPPC and DMPC has been determined using several techniques
25 under different experimental conditions because of their accessible T_m values (in
26 MLVs, $T_m=23.5$ °C for DMPC and 41.4 °C for DPPC²⁸). Table S1 summarizes a
27 compilation of the reported data on different solids using LB-LS or vesicle rupture
28 (VR) deposition methods.
29

30 In agreement with the proposed loss in entropy, most of the experimental T_m
31 values are higher than those of MLVs (see Table S1). However, this is not
32 observed in all cases and there is a great variability in the measured T_m values
33 which can be explained by considering the extreme sensitivity of bilayer dynamics
34 to multiple parameters as: i) the chemical nature of the support (glass, mica, silicon
35 oxide, etc) as well as their chemical properties, derived from different pre-
36 treatment, leading to different roughness, hydrophobicity and wettability.⁴⁵ ii) the
37 manner in which the film was formed on the support (LB-LS or the rupture of
38 vesicles^{29,30}), probably leading to films of different density and/or different thickness
39 of the water cleft. iii) the temperature and the ionic strength of the system at the
40 transferring stage^{6,31,32}.
41

42 For bilayers on mica, a decoupling of the hemilayers has been measured,
43 with two different melting values and two different diffusion coefficients.^{29,31–34} This
44 decoupled phase transition was proposed to be a result of the strong interaction
45 between the proximal lipid hemilayer and the support, with the mica surface
46 stabilizing the solid phase of the proximal monolayer through electrostatic
47 interactions resulting in dehydration of the lipid headgroups.³³ Supporting this idea,
48 the phase transition on mica has been turned to a coupled transition by changing
49 the ionic strength of the aqueous milieu.³² Contrary to mica surfaces, we and other
50 authors^{26,29,35} found that, on glass or a silicon oxide, there was no distinction
51
52
53
54
55
56
57
58
59
60

1
2
3 between the distal and proximal leaflets, suggesting a weaker interaction between
4 the lipid film and these surfaces, probably related with the higher roughness of the
5 latter.
6
7

8
9 Regarding the manner in which the transition process occurs, it is known
10 that the main transition in pure lipid water suspensions is a highly cooperative
11 endothermic process with peak widths of $<0.1^{\circ}\text{C}$ at slow scanning rates.³⁶ In SLBs
12 the phase transitions are less cooperative, with reported temperature widths
13 between 2°C and 10°C (see Table S1) and the causes of this behavior remain
14 unclear. On this subject, it has been reported that in vesicles with single bilayers
15 (which are more comparable to SLBs than MLV) the cooperativity decreases
16 compared to multilayers.^{37–39} While it is known that in free-standing bilayers the
17 gel-to-fluid transition takes place at constant surface pressure with increments in
18 the lipids molecular areas, there still is an attempt to answer the question if the
19 phase transition in SLBs take place at constant surface pressure with area
20 expansion, or at constant area with variation of the surface pressure, or neither of
21 them. Charrier and Thibaudau²⁴ have proposed a model that supports a quasi-
22 constant area phase transition, while this assumption was questioned by
23 Ramkaran and Badia.³¹
24
25
26
27

28 In Langmuir monolayers, it is possible to fix one of the parameters (area or
29 surface pressure) while varying the temperature of the film (for details see SM).
30 Therefore, we evaluated the phase transition of monolayers of DPPC and DMPC at
31 each condition and found that the temperature range where phase transition
32 occurred was larger when the area was fixed ($\sim 14^{\circ}\text{C}$) than when the fixed
33 parameter was surface pressure ($\sim 6^{\circ}\text{C}$), in which case the range was similar to the
34 reported values (Table S1), supporting the idea of a phase transition with a
35 variable molecular area as proposed by Ramkaran and Badia.³¹ This matches
36 observations using AFM to image SLBs, where an expansion of the film and a
37 filling of the defects with membrane while increasing the temperature have been
38 described, and also matches diffusion experiments, which show that the lipid
39 molecules are not pinned down to the surface but may expand across it.^{29,33,35,40–42}
40
41
42
43
44

45 5. Conclusions

46 Here we presented a novel method for the determination of the chemical
47 potential difference involved in the phase transition of pure lipids that may be
48 applied to different model membranes. Using this approach, we were able to
49 estimate the free energy change for the phase transition of five phospholipids
50 differing in the hydrocarbon chain length in LMs and SLBs and thereby a
51 comparison of the energetic cost for the condensing process (from liquid-expanded
52 to liquid-condensed states) in the presence and in the absence of a solid wall was
53 performed. The results showed that the energy involved in the phase transition of
54 lipids arranged in supported films was lower than for free-standing films, and thus,
55
56
57
58
59
60

1
2
3 the phases become more similar to each other when closer to a solid confinement.
4 This effect may be caused by a change in the entropy of the process, the enthalpy,
5 or both. In any case, the energetic change was not related with an ordering effect
6 of the hydrocarbon chain and was a long-range effect, probably related with the
7 impediment of the out-of-plane motion of the film by the solid surface.
8

9
10 In summary, even in the absence of strong film-surface interactions, our
11 results indicate that a solid support induces a reduction of the energy gap between
12 the different phase states, which translates to changes on the phase diagram
13 corresponding to membranes with more than one component.
14

15 16 17 **Acknowledgments** 18

19
20 This work was supported by SECyT-UNC, CONICET and FONCYT (Program BID
21 PICT 2012-0344) Argentina. N.W. is a Career Investigator and A.M. is a fellow of
22 CONICET.
23
24

25 26 **Supporting Information** 27

28
29 Table S1: Summary of published melting temperatures for DMPC and DPPC.
30 Experimental details for the constant area/surface pressure phase transition
31 assays.
32 This information is available free of charge via the Internet at (<http://pubs.acs.org>).
33
34
35
36
37
38
39
40
41
42
43
44
45
46
47
48
49
50
51
52
53
54
55
56
57
58
59
60

REFERENCES

- (1) Sackmann, E. Supported Membranes: Scientific and Practical Applications. *Science* **1996**, *271* (January), 43–48.
- (2) Castellana, E. T.; Cremer, P. S. Solid Supported Lipid Bilayers: From Biophysical Studies to Sensor Design. *Surf. Sci. Rep.* **2006**, *61*, 429–444.
- (3) Kalb, E.; Frey, S.; Tamm, L. K. Formation of Supported Planar Bilayers by Fusion of Vesicles to Supported Phospholipid Monolayers. *Biochim. Biophys. Acta - Biomembr.* **1992**, *1103*, 307–316.
- (4) Crane, J. M.; Kiessling, V.; Tamm, L. K. Measuring Lipid Asymmetry in Planar Supported Bilayers by Fluorescence Interference Contrast Microscopy. *Langmuir* **2005**, *21* (15), 1377–1388.
- (5) Lin, W.-C.; Blanchette, C. D.; Ratto, T. V.; Longo, M. L. Lipid Asymmetry in DLPC/DSPC-Supported Lipid Bilayers: A Combined AFM and Fluorescence Microscopy Study. *Biophys. J.* **2006**, *90* (1), 228–237.
- (6) Wacklin, H. P. Composition and Asymmetry in Supported Membranes Formed by Vesicle Fusion. *Langmuir* **2011**, *27*, 7698–7707.
- (7) Mangiarotti, A.; Caruso, B.; Wilke, N. Phase Coexistence in Films Composed of DLPC and DPPC: A Comparison between Different Model Membrane Systems. *Biochim. Biophys. Acta - Biomembr.* **2014**, *1838* (7), 1823–1831.
- (8) Tokumasu, F.; Jin, A. J.; Feigenson, G. W.; Dvorak, J. a. Nanoscopic Lipid Domain Dynamics Revealed by Atomic Force Microscopy. *Biophys. J.* **2003**, *84* (4), 2609–2618.
- (9) Gaines, G. L. *Insoluble Monolayers at Liquid-Gas Interfaces*; Interscience Publishers: New York, 1966.
- (10) Caruso, B.; Mangiarotti, A.; Wilke, N. Stiffness of Lipid Monolayers with Phase Coexistence. *Langmuir* **2013**, *29* (34), 10807–10816.
- (11) Mercado, F. V.; Maggio, B.; Wilke, N. Phase Diagram of Mixed Monolayers of Stearic Acid and Dimyristoylphosphatidylcholine. Effect of the Acid Ionization. *Chem. Phys. Lipids* **2011**, *164* (5), 386–392.
- (12) Rosetti, C. M.; Wilke, N.; Maggio, B. Thermodynamic Distribution Functions Associated to the Isothermal Phase Transition in Langmuir Monolayers. *Chem. Phys. Lett.* **2006**, *422*, 240–245.

- 1
2
3 (13) Xing, C.; Faller, R. *What Is the Difference between a Supported and a Free*
4 *Bilayer? Insights from Molecular Modeling on Different Scales*, 1st ed.;
5 Elsevier Inc., 2010; Vol. 11.
6
7
8 (14) Barneveld, P. a; Scheutjens, J. M. H. M.; Lyklema, J. Bending Moduli and
9 Spontaneous Curvature. 1. Bilayers and Monolayers of Pure and Mixed
10 Nonionic Surfaatants. *Langmuir* **1992**, *8* (7), 3122–3130.
11
12 (15) Baoukina, S.; Monticelli, L.; Risselada, H. J.; Marrink, S. J.; Tieleman, D. P.
13 The Molecular Mechanism of Lipid Monolayer Collapse. *Proc. Natl. Acad.*
14 *Sci. U. S. A.* **2008**, *105* (31), 10803–10808.
15
16 (16) Helm, C. a; Möhwald, H.; Kjær, K.; Als-Nielsen, J. Phospholipid Monolayer
17 Density Distribution Perpendicular to the Water Surface. A Synchrotron X-
18 Ray Reflectivity Study. *Europhys. Lett.* **2007**, *4*, 697–703.
19
20 (17) Braslau, a.; Deutsch, M.; Pershan, P. S.; Weiss, a. H.; Als-Nielsen, J.; Bohr,
21 J. Surface Roughness of Water Measured by X-Ray Reflectivity. *Phys. Rev.*
22 *Lett.* **1985**, *54* (2), 114–117.
23
24 (18) Heberle, F. a.; Pan, J.; Standaert, R. F.; Drazba, P.; Kucerka, N.; Katsaras,
25 J. Model-Based Approaches for the Determination of Lipid Bilayer Structure
26 from Small-Angle Neutron and X-Ray Scattering Data. *Eur. Biophys. J.* **2012**,
27 *41*, 875–890.
28
29 (19) Bayerl, T. M.; Bloom, M. Physical Properties of Single Phospholipid Bilayers
30 Adsorbed to Micro Glass Beads. A New Vesicular Model System Studied by
31 2H-Nuclear Magnetic Resonance. *Biophys. J.* **1990**, *58* (August), 357–362.
32
33 (20) Johnson, S. J.; Bayerl, T. M.; McDermott, D. C.; Adam, G. W.; Rennie, a R.;
34 Thomas, R. K.; Sackmann, E. Structure of an Adsorbed
35 Dimyristoylphosphatidylcholine Bilayer Measured with Specular Reflection of
36 Neutrons. *Biophys. J.* **1991**, *59* (2), 289–294.
37
38 (21) Kim, J.; Kim, G.; Cremer, P. S. Investigations of Water Structure at the
39 Solid/liquid Interface in the Presence of Supported Lipid Bilayers by
40 Vibrational Sum Frequency Spectroscopy. *Langmuir* **2001**, *17* (23), 7255–
41 7260.
42
43 (22) Gov, N.; Zilman, a. G.; Safran, S. Hydrodynamics of Confined Membranes.
44 *Phys. Rev. E - Stat. Nonlinear, Soft Matter Phys.* **2004**, *70* (October 2003),
45 1–10.
46
47 (23) Hoopes, M. I.; Deserno, M.; Longo, M. L.; Faller, R. Coarse-Grained
48 Modeling of Interactions of Lipid Bilayers with Supports. *J. Chem. Phys.*
49 **2008**, *129* (2008).
50
51
52
53
54
55
56
57
58
59
60

- 1
2
3 (24) Charrier, A.; Thibaudau, F. Main Phase Transitions in Supported Lipid
4 Single-Bilayer. *Biophys. J.* **2005**, *89* (August), 1094–1101.
5
6
7 (25) Xing, C.; Faller, R. Interactions of Lipid Bilayers with Supports: A Coarse-
8 Grained Molecular Simulation Study. *J. Phys. Chem. B* **2008**, *112*, 7086–
9 7094.
10
11 (26) Seeger, H. M.; Cerbo, A. D.; Alessandrini, A.; Facci, P. Supported Lipid
12 Bilayers on Mica and Silicon Oxide: Comparison of the Main Phase
13 Transition Behavior. *J. Phys. Chem. B* **2010**, *114*, 8926–8933.
14
15
16 (27) Tokumasu, F.; Jin, A. J.; Dvorak, J. a. Lipid Membrane Phase Behaviour
17 Elucidated in Real Time by Controlled Environment Atomic Force
18 Microscopy. *J. Electron Microsc. (Tokyo)*. **2002**, *51* (1), 1–9.
19
20
21 (28) Marsh, D. *Handbook of Lipid Bilayers*; CRC Press: Boca Raton, FL, 1990.
22
23
24 (29) Scomparin, C.; Lecuyer, S.; Ferreira, M.; Charitat, T.; Tinland, B. Diffusion in
25 Supported Lipid Bilayers: Influence of Substrate and Preparation Technique
26 on the Internal Dynamics. *Eur. Phys. J. E* **2009**, *28*, 211–220.
27
28
29 (30) Richter, R. P.; Bérat, R.; Brisson, A. R. Formation of Solid-Supported Lipid
30 Bilayers: An Integrated View. *Langmuir* **2006**, *22* (12), 3497–3505.
31
32 (31) Ramkaran, M.; Badia, A. Gel-to-Fluid Phase Transformations in Solid-
33 Supported Phospholipid Bilayers Assembled by the Langmuir-Blodgett
34 Technique: Effect of the Langmuir Monolayer Phase State and Molecular
35 Density. *J. Phys. Chem. B* **2014**, *118*, 9708–9721.
36
37
38 (32) Seeger, H. M.; Marino, G.; Alessandrini, a.; Facci, P. Effect of Physical
39 Parameters on the Main Phase Transition of Supported Lipid Bilayers.
40 *Biophys. J.* **2009**, *97* (4), 1067–1076.
41
42 (33) Keller, D.; Larsen, N. B.; Møller, I. M.; Mouritsen, O. G. Decoupled Phase
43 Transitions and Grain-Boundary Melting in Supported Phospholipid Bilayers.
44 *Phys. Rev. Lett.* **2005**, *94* (January), 1–4.
45
46
47 (34) Feng, Z. V.; Spurlin, T. a; Gewirth, A. a. Direct Visualization of Asymmetric
48 Behavior in Supported Lipid Bilayers at the Gel-Fluid Phase Transition.
49 *Biophys. J.* **2005**, *88* (3), 2154–2164.
50
51
52 (35) Tamm, L. K.; McConnell, H. M. Supported Phospholipid Bilayers. *Biophys. J.*
53 **1985**, *47* (1), 105–113.
54
55
56 (36) Knoll, W. Calorimetric Invesstigations of Lipid Phase Transitions. I. The
57 Width of Transition. *Thermochim. Acta* **1984**, *77*, 35–47.
58
59
60

- 1
2
3 (37) Leonenko, Z. V; Finot, E.; Ma, H.; Dahms, T. E. S.; Cramb, D. T.
4 Investigation of Temperature-Induced Phase Transitions in DOPC and DPPC
5 Phospholipid Bilayers Using Temperature-Controlled Scanning Force
6 Microscopy. *Biophys. J.* **2004**, *86* (June), 3783–3793.
7
8
9 (38) Biltonen, R. L.; Lichtenberg, D. The Use of Differential Scanning Calorimetry
10 as a Tool to Characterize Liposome Preparations. *Chem. Phys. Lipids* **1993**,
11 *64*, 129–142.
12
13 (39) Carnini, A.; Phillips, H. a; Shamrakov, L. G.; Cramb, D. T. Revisiting Lipid
14 General Anesthetic Interactions (II): Halothane Location and Changes in
15 Lipid Bilayer Microenvironment Monitored by Fluorescence. *Can. J. Chem.*
16 **2004**, *82* (li), 1139–1149.
17
18
19 (40) Yarrow, F.; Kuipers, B. W. M. AFM Study of the Thermotropic Behaviour of
20 Supported DPPC Bilayers with and without the Model Peptide WALP23.
21 *Chem. Phys. Lipids* **2011**, *164* (1), 9–15.
22
23
24 (41) Xie, A. F.; Yamada, R.; Gewirth, A. a; Granick, S. Materials Science of the
25 Gel to Fluid Phase Transition in a Supported Phospholipid Bilayer. *Phys.*
26 *Rev. Lett.* **2002**, *89*, 246103.
27
28
29 (42) Tokumasu, F.; Jin, A. J.; Feigenson, G. W.; Dvorak, J. a. Atomic Force
30 Microscopy of Nanometric Liposome Adsorption and Nanoscopic Membrane
31 Domain Formation. *Ultramicroscopy* **2003**, *97*, 217–227.
32
33
34
35
36
37
38
39
40
41
42
43
44
45
46
47
48
49
50
51
52
53
54
55
56
57
58
59
60

Table of Contents (TOC):

